Journal of Molecular Catalysis A: Chemical 367 (2013) 12–22

Contents lists available at SciVerse ScienceDirect

Journal of Molecular Catalysis A: Chemical

journal homepage: www.elsevier.com/locate/molcata

Mg–Al hydrotalcite as an efficient catalyst for microwave assisted regioselective 1,3-dipolar cycloaddition of nitrilimines with the enaminone derivatives: A green protocol

Tamer S. Saleh, Katabathini Narasimharao, Nesreen S. Ahmed, Sulaiman N. Basahel, Shaeel A. Al-Thabaiti, Mohamed Mokhtar*

Chemistry Department, Faculty of Science, King Abdulaziz University, Jeddah 21589, Saudi Arabia

ARTICLE INFO

Article history:
Received 5 October 2012
Received in revised form
11 November 2012
Accepted 13 November 2012
Available online xxx

Keywords:
1,3-Dipolar cycloaddition
Regioselectivity
Enaminones
Nitrilimines
Microwave irradiation
Mg–Al hydrotalcite

ABSTRACT

Microwave assisted generation of in situ nitrilimines and their regioselective 1,3-dipolar cycloaddition reaction with enaminones to produce pyrazole derivatives by Mg–Al hydrotalcite (Mg–Al HT) catalyst is introduced. Short reaction times with high yields (90–94%), the absence of an organic solvent and reuse of the catalyst for at least five times without loss of activity could regard as cost effective, environmentally friendly and greener process. The fresh and used catalysts were characterized by X-ray diffraction (XRD), Fourier transform infrared (FTIR), Raman spectroscopy, N_2 physisorption and temperature programmed desorption by CO_2 (CO_2-TPD) to understand the role of hydrotalcite in the reaction mechanism and the robust nature of the catalyst. It appears that better microwave absorptivity of the catalyst with Mg–Al HT structure might be responsible for shorter reaction times with high yields. A plausible mechanism for 1,3-dipolar cycloaddition over the Mg–Al HT is proposed.

1. Introduction

Synthesis of pyrazole derivatives has still been an active area of research due its prominent structure motif found in numerous pharmaceutically active compounds [1]. Pyrazole framework plays an essential role in biologically active compounds and therefore represents an interesting template for combinatorial as well as medicinal chemistry [2–5]. The pyrazole nucleus is a ubiquitous feature of fertile source of medicinal agents such as antimicrobial [6], antiviral [7,8] and anticancer [9,10] agents specially after the discovery of the natural pyrazole C-glycoside pyrazofurin; 4-hydroxy-3-β-D-ribofuranosyl-1*H*-pyrazole-5-carboxamide (Fig. 1) [11].

One of the most important method used for synthesis of pyrazole derivatives is 1,3-dipolar cycloaddition (1,3-DC) utilizing nitrilimine (generated in situ by the action of base on the hydrazonoyl halide) and α,β-unsaturated carbonyl compounds (Scheme 1) [12,13]. Huisgen [14] first reported the dehydrohalogenation of hydrazidic halides under mild conditions (benzene solution with triethylamine as catalyst) is a convenient route to synthesize 1,3-di-substituted nitrilimines. Later on, many research groups [15] used different homogeneous and heterogeneous catalysts for 1,3-DC of 1,3-dipoles with π-electronic deficient moieties to synthesize five or six membered heterocyclic compounds. Recently, Tseng et al. [16] have developed new method for one-pot 1,3-DC to prepare a series of 3,5-disubstituted 1,2,4-triazole compounds by reacting various aldehydes with hydrazonoyl hydrochlorides in the presence of hydroxylamine hydrochloride as a functionality transferring reagent, triethylamine as a basic catalyst and toluene as solvent.

However, these homogeneous methodologies are suffering from disadvantages mainly, use of homogeneous base such as triethylamine and non-polar solvent such as benzene, which are undesirable from an environmental point of view and also these reactions generate considerable amounts of wasteful salts. In recent years, researchers are dedicating their efforts to find alternative methodologies for waste minimization in fine chemicals and drugs manufacturing processes by replacing the stoichiometric organic synthesis methodologies, which uses large amounts of inorganic and organic reagents with cleaner, catalytic methodologies [17].

A deep search in the literature revealed a lack of general investigation on utilization of heterogeneous catalysts for 1,3-DC reaction. For the first time, Broggini et al. [18] reported the application of Ag_2CO_3 as a promoter in heterogeneous reaction conditions for

* Corresponding author. Tel.: +966 500558045; fax: +966 26952292.
E-mail address: mmokhtar2000@yahoo.com (M. Mokhtar).

1381-1169/$ – see front matter © 2012 Elsevier B.V. All rights reserved.
http://dx.doi.org/10.1016/j.molcata.2012.11.009

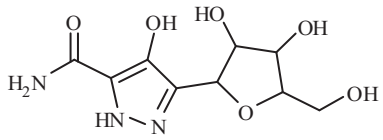

Fig. 1. Structure of pyrazofurin.

in situ generation of nitrile iminies from hydrazononyl halides. They observed that the reaction between hydrazononyl chlorides and allylic alcohols in the presence of Ag_2CO_3 exhibits different features than in the presence of conventional bases such as tertiary amines. Later, Bonini et al. [19] used Ag_2CO_3 as a base along with $Sc(OTf)_3$ for the 1,3-DC of nitrile imines with functionalized acetylenes. The same group extended the application of the same methodology to the regiocontrolled synthesis of thieno[2,3-*c*]-pyrazoles through 1,3-DC of nitrile imines and substituted acetylenes bearing thiol or sulfone groups [19]. 1,3-Dipolar ions have been shown to undergo a wide variety of cycloadditions usually in situ, but the mechanism of this process remains controversial [20].

In recent years, hydrotalcites (HTs) have found applications in various base catalyzed reactions including [3 + 2] cycloaddition reactions that are used for the synthesis of isoxazoles and tetrazoles [21]. Due to its ability of altering the nature of the basic sites by the preparation conditions, HTs showed great potential in the reactions that required Lewis basic sites, Brönsted basic sites or even pairs of acid–base sites [22]. The use of microwave irradiation in organic synthesis has become increasingly popular within the pharmaceutical and academic arenas, because it is a new enabling technology for drug discovery and development [23]. Taking the advantage of this efficient source of energy (enhances reaction rates, high yields, improved purity, ease of work up after the reaction and eco-friendly reaction conditions compared to the conventional methods), compound libraries for lead generation and optimization can be assembled in a fraction of the time required by classical thermal methods. Kaddar et al. [24] studied the 1,3-DC activity of hydrazonoyl chlorides over Al_2O_3 with various alkenes and alkynes under microwave irradiation. They observed that the microwave heating accelerates the cycloaddition process when the reaction performed in non-polar solvent, but the yields are relatively low for the investigated substrates (maximum 50%). The lower yields of the products could be related to the lower basic strength of the Al_2O_3 catalyst. Motivated by the aforementioned findings, and in a continuation of our interest in synthesis of a wide range of heterocyclic systems for biological screening program in our laboratory [25], also, as a part of our program toward the non-conventional approach to the experimental set up of organic reactions [26], the concept of "Microwave induced Organic Reaction Enhancement" (MORE) chemistry has been utilized for rapid and sustainable regioselective synthesis of some pyrazole derivatives. Here we are reporting a green protocol, which does not generate any harmful and/or wasteful co-products via using recyclable solid Mg–Al HT catalyst for in situ generation of nitrilimine and subsequent 1,3-DC with enaminone derivatives. To best of our knowledge, the application of Mg–Al HT catalysts for the aforementioned reaction has not previously been reported. A detailed characterization of fresh and spent catalysts has been carried out to understand the role and stability of HT structure.

2. Experimental

2.1. Preparation of catalysts

Mg–Al (3:1) HT catalyst was prepared by following the procedure reported in our previous publication [27]. Synthetic HT was prepared by co-precipitation using two solutions (A) and (B). Solution (A) contained the desired amount of Mg and Al nitrates and solution (B) consisted of the precipitating agents NaOH and Na_2CO_3. Within 5 min the two solutions were added simultaneously into the reaction vessel while the pH was maintained at ca. 10 under vigorous stirring at 30 °C for 17 h by ultrasound. Finally, the sample was washed by dispersion in distilled water under gentle stirring followed by filtration. This washing/filtration step was repeated five times till the precipitate was free from sodium ions as confirmed from ICP analyses. The precipitate was dried at 80 °C for 12 h. For calcination the as-synthesized HT sample was heated under the flow of air for 3 h at 450 °C in a muffle furnace.

2.2. Characterization of catalysts

X-ray powder diffraction (XRD) studies were performed for all the prepared solid samples using a Bruker diffractometer (Bruker D8 advance target). The patterns were run with Cu Kα with secondly monochromator (λ = 1.5405 Å) at 40 kV and 40 mA. The identification of different crystalline phases in the samples was performed by comparing the data with the Joint Committee for Powder Diffraction Standard (JCPDS) files. FTIR spectra of catalysts were recorded using Shimadzu FT-IR 8101 PC infrared spectrophotometer. The Raman spectra of samples were measured with a Bruker Equinox 55 FT-IR spectrometer equipped with a FRA106/S FT-Raman module and a liquid N_2 cooled Ge detector, using the 1064 nm line of an Nd:YAG laser with an output laser power of 200 mW. Textural properties of the prepared samples were determined from nitrogen adsorption/desorption isotherms measurements at −196 °C using Autosorb iQ automated gas sorption system 70 (Quantachrome, USA). The specific surface area, S_{BET}, was

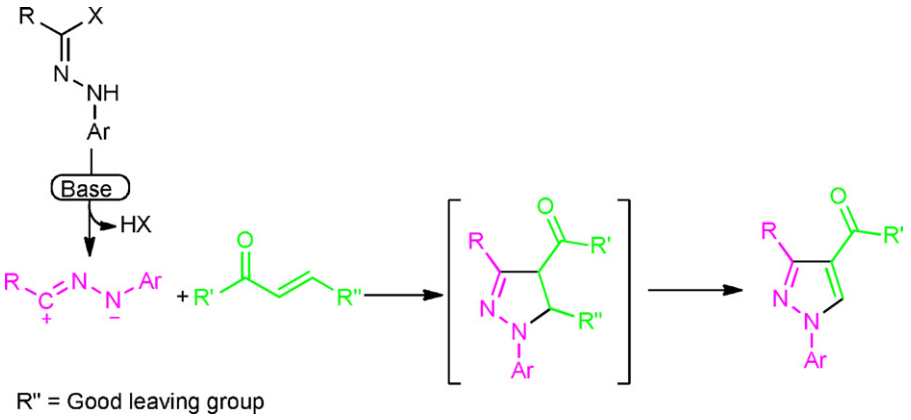

Scheme 1. 1,3-Dipolar cycloaddation protocol via nitrilimines and α,β-unsaturated carbonyl compounds.

calculated by applying the Brunauer–Emmett–Teller (BET) equation. Pore size distribution over the mesopore range was generated by the Barrett–Joyner–Halenda (BJH) analysis of the desorption branches, and values of the average pore size were calculated. CO_2-TPD patterns were recorded using Chembet-3000 (Quantachrome, USA).

2.3. Synthesis of pyrazole derivatives, **5a–f**

2.3.1. Microwave irradiation method

Mg–Al HT (0.5 g) was added to an enaminone derivative **3** (10 mmol) and the appropriate hydrazonyl chloride **1a–c** (10 mmol) in a mortar, and the mixture was grounded thoroughly with a pestle at room temperature. The total mixture was placed in a Teflon process vial and it was irradiated by microwaves with power of 330 W to reach a reaction temperature of 120 °C under auto generated pressure. The vial was exposed to microwaves for a required time to complete the reaction. The progress of the reaction was monitored by TLC for every 1 min (eluent; petroleum ether: chloroform). Upon completion of the reaction, the mixture was cooled and the product was extracted by dissolution in ethanol. The catalyst was removed by filtration and washed with hot ethanol and the solvent was evaporated under reduced pressure to obtain the solid product. The obtained solid product was purified by crystallization using ethanol/dimethyl formamide solvent mixture to afford the pure pyrazole derivatives **5a–f** in excellent yields. Compound **5a** was obtained by using various heterogeneous catalysts (basic alumina, KF/basic alumina, K_2CO_3, MgO, Mg: Al-HT and also in neat conditions (without catalyst) under microwave irradiation.

2.3.2. Conventional electrical heating method

The reactions were performed on the same scale as described above. The reactants and catalyst were put in a flask then sealed with a rubber septum. The reaction mixture was heated at 120 °C on a thermostatic oil-bath for required time to complete the reaction as monitored by TLC. After the completion of the reaction, the reaction mixture was cooled to room temperature and the products were obtained and purified as described in the previous method.

Physical and spectral data of the compounds **5a–f** are listed below.

*2.3.2.1. 3-Acetyl-4-benzoyl-1-phenylpyrazole (**5a**).* mp. 141–143 °C, IR (KBr) ν_{max}/cm^{-1}: 1695, 1652 (2C=O), 1602 (C=N), ^{1}H NMR ($CDCl_3$): δ 2.69 (s, 3H, CH_3), 7.23–7.92 (m, 10H, ArH's), 8.11 (s, 1H, pyrazole-5-CH), ^{13}C NMR ($CDCl_3$): δ 26.11, 110.55, 121.22, 127.54, 128.08, 128.09, 129.68, 129.69, 130.65, 132.87, 138.54, 146.32, 189.94, 195.75, MS (*m*/*z*): 290 (M^+), Anal. Calcd for $C_{18}H_{14}N_2O_2$ (290.31): C, 74.47; H, 4.86; N, 9.65%. Found: C, 74.61; H, 4.81; N, 9.56%.

*2.3.2.2. 3-Acetyl-4-(4-flurobenzoyl)-1-phenylpyrazole (**5b**).* mp. 130–132 °C, IR (KBr) ν_{max}/cm^{-1}: 1680, 1644 (2C=O), 1594 (C=N), ^{1}H NMR ($CDCl_3$): δ 2.66 (s, 3H, CH_3), 7.55–7.81 (m, 9H, ArH's), 8.22 (s, 1H, pyrazole-5-CH), ^{13}C NMR ($CDCl_3$): δ 27.14, 119.88, 123.33, 128.37, 128.41, 129.82, 130.21, 130.73, 131.76, 136.72, 138.91, 150.38 189.24, 192.93, MS (*m*/*z*): 308 (M^+), Anal. Calcd for $C_{18}H_{13}FN_2O_2$ (308.31): C, 70.12; H, 4.25; N, 9.09%. Found: C, 70.33; H, 4.16; N, 8.97%.

*2.3.2.3. 3-Acetyl-4-benzoyl-1-(4-flurophenyl)pyrazole (**5c**).* mp. 148 °C, IR (KBr) ν_{max}/cm^{-1}: 1685, 1643 (2C=O), 1594 (C=N), ^{1}H NMR ($CDCl_3$): δ 2.68 (s, 3H, CH_3), 7.10–7.81 (m, 9H, ArH's), 8.41 (s, 1H, pyrazole-5-CH), ^{13}C NMR ($CDCl_3$): δ 27.04, 112.56, 117.29, 117.30, 119.72, 119.73, 127.11, 128.58, 129.79, 129.80, 131.04, 134.78, 137.37, 147.00, 160.01, 190.59, 194.98, MS (*m*/*z*): 308 (M^+), Anal. Calcd for $C_{18}H_{13}FN_2O_2$ (308.31): C, 70.12; H, 4.25; N, 9.09%. Found: C, 70.28; H, 4.19; N, 8.99%.

*2.3.2.4. 3-Acetyl-4-(4-flurobenzoyl)-1-(4-flurophenyl)pyrazole (**5d**).* mp. 162–164 °C, IR (KBr) ν_{max}/cm^{-1}: 1686, 1654 (2C=O), 1592 (C=N), ^{1}H NMR ($CDCl_3$): δ 2.66 (s, 3H, CH_3), 7.25–7.87 (m, 8H, ArH's), 8.45 (s, 1H, pyrazole-5-CH), ^{13}C NMR ($CDCl_3$): δ 26.95, 111.84, 113.12, 113.13, 116.21, 116.22, 119.44, 128.00, 1287.79, 133.06, 133.07, 144.62, 159.98, 161.11, 191.54, 193.90. MS (*m*/*z*): 326 (M^+), Anal. Calcd for $C_{18}H_{12}F_2N_2O_2$ (326.30): C, 66.26; H, 3.71; N, 8.59%. Found: C, 66.51; H, 3.61; N, 8.44%.

*2.3.2.5. 3-Acetyl-4-benzoyl-1-(4-trifluromethylphenyl)pyrazole (**5e**).* mp. 177 °C, IR (KBr) ν_{max}/cm^{-1}: 1692, 1658 (2C=O), 1599 (C=N), ^{1}H NMR ($CDCl_3$): δ 2.59 (s, 3H, CH_3), 7.15–7.76 (m, 9H, ArH's), 8.36 (s, 1H, pyrazole-5-CH), ^{13}C NMR ($CDCl_3$): δ 26.25, 111.02, 119.54, 119.55, 122.00, 126.55, 127.84, 127.85, 128.56, 130.02, 133.46, 134.75, 146.33, 147.18, 192.56, 195.07. MS (*m*/*z*): 358 (M^+). Anal. Calcd for $C_{19}H_{13}F_3N_2O_2$ (358.31): C, 63.69; H, 3.66; N, 7.28%. Found: C, 63.96; H, 3.53; N, 7.14%.

*2.3.2.6. 3-Acetyl-4-(4-flurobenzoyl)-1-(4-trifluromethylphenyl)pyrazole (**5f**).* mp. 158 °C, IR (KBr) ν_{max}/cm^{-1}: 1698, 1659 (2C=O), 1592 (C=N), ^{1}H NMR ($CDCl_3$): δ 2.63 (s, 3H, CH_3), 7.09–7.84 (m, 8H, ArH's), 8.52 (s, 1H, pyrazole-5-CH), ^{13}C NMR ($CDCl_3$): δ 26.45, 112.23, 116.02, 119.54, 122.62, 126.33, 126.34, 128.04, 128.98, 130.38, 130.39, 139.45, 144.08, 161.21, 191.27, 194.06. MS (*m*/*z*): 376 (M^+). Anal. Calcd for $C_{19}H_{12}F_4N_2O_2$ (376.30): C, 60.64; H, 3.21; N, 7.44%. Found: C, 60.93; H, 3.06; N, 7.30%.

2.4. Synthesis of pyrazolo[3,4-d]pyridazine derivatives, **8a–f**

2.4.1. Microwave irradiation method

To a solution of appropriate pyrazole derivatives **5a–f** (1 mmol) in ethanol (2 mL), hydrazine hydrate (98%), (2 mL, 10 mmol) was added in a process vial. The vial was capped properly and irradiated by microwaves with a power of 330 W to reach reaction temperature, 120 °C. The progress of the reaction was monitored by TLC for every 1 min. The solid reaction product was removed from vial and washed with ethanol and recrystallized using dimethyl formamide (DMF) solvent to afford the corresponding pyrazolo[3,4-*d*]pyridazine derivatives **8a–f**.

2.4.2. Conventional electrical heating method

A mixture of the pyrazole derivative **5a–f** (1 mmol) and hydrazine hydrate (98%), (2 mL, 10 mmol) was refluxed in ethanol (20 mL) under electrical heating for 1 h and then left to cool to room temperature. The formed precipitates were collected by filtration, washed with ethanol and dried. Recrystallization using DMF afforded yellow crystals of the corresponding pyrazolo[3,4-*d*]pyridazine derivatives **8a–f**.

Physical and spectral data of the compounds **8a–f** listed below.

*2.4.2.1. 7-Methyl-2,4-diphenyl-2H-pyrazolo[3,4-d]pyridazine (**8a**).* mp. 239 °C, IR (KBr) ν_{max}/cm^{-1}: 1596 (C=N), ^{1}H NMR (DMSO-d_6): δ 2.96 (s, 3H, CH_3), 7.18–7.82 (m, 10H, ArH's), 8.76 (s, ^{1}H-pyrazole), ^{13}C NMR (DMSO-d_6): δ 17.93, 110.23, 121.38, 124.54, 126.41, 126.42, 128.41, 129.85, 129.86, 129.97, 133.85, 141.12, 142.48, 148.04, 152.00, 154.20. MS (*m*/*z*): 286 (M^+). Anal. Calcd for $C_{18}H_{14}N_4$ (286.32): C, 75.51; H, 4.92; N, 19.57%. Found: C, 75.83; H, 4.77; N, 19.40%.

*2.4.2.2. 4-(4-Fuorophenyl)-7-methyl-2-phenyl-2H-pyrazolo[3,4-d]pyridazine (**8b**).* mp. 251 °C, IR (KBr) ν_{max}/cm^{-1}: 1593 (C=N), ^{1}H NMR (DMSO-d_6): δ 2.82 (s, 3H, CH_3), 7.25–7.95 (m, 9H, ArH's), 8.68

(s, ^{1}H-pyrazole), ^{13}C NMR (DMSO-d_6): δ 17.56, 109.89, 113.33, 120.07, 120.08, 123.57, 127.54, 128.49, 128.50, 130.25, 132.47, 138.05, 141.00, 148.32, 153.10, 162.33. MS (*m*/*z*): 304 (M^+). Anal. Calcd for $C_{18}H_{13}FN_4$ (304.32): C, 71.04; H, 4.31; N, 18.41%. Found: C, 71.36; H, 4.17; N, 18.24%.

*2.4.2.3. 2-(4-Fluorophenyl)-7-methyl-4-phenyl-2H-pyrazolo[3,4-d]pyridazine (**8c**).* mp. 276 °C, IR (KBr) ν_{max}/cm^{-1}: 1599 (C=N), ^{1}H NMR (DMSO-d_6): δ 2.89 (s, 3H, CH_3), 7.69–8.12 (m, 9H, ArH's), 8.66 (s, ^{1}H-pyrazole), ^{13}C NMR (DMSO-d_6): δ 17.91, 111.58, 116.25, 116.26, 119.01, 123.89,123.90, 127.01, 128.63, 128.64, 131.98, 134.00, 134.75, 139.59, 148.09, 152.66, 163.84. MS (*m*/*z*): 304 (M^+). Anal. Calcd for $C_{18}H_{13}FN_4$ (304.32): C, 71.04; H, 4.31; N, 18.41%. Found: C, 71.29; H, 4.20; N, 18.27%.

*2.4.2.4. 2,4-Bis(4-fluorophenyl)-7-methyl-2H-pyrazolo[3,4-d]pyridazine(**8d**).* mp. >300 °C, IR (KBr) ν_{max}/cm^{-1}: 1595 (C=N), ^{1}H NMR (DMSO-d_6): δ 2.78 (s, 3H, CH_3), 7.13–7.82 (m, 8H, ArH's), 8.71 (s, ^{1}H-pyrazole), ^{13}C NMR (DMSO-d_6): δ 17.15, 110.18, 114.98, 114.99, 118.00, 118.01, 123.89,125.10, 128.06, 128.64, 128.65, 133.08, 139.18, 147.96, 151.54, 163.54, 165.00. MS (*m*/*z*): 322 (M^+). Anal. Calcd for $C_{18}H_{12}F_2N_4$ (322.31): C, 67.08; H, 3.75; N, 17.83%. Found: C, 67.35; H, 3.62; N, 17.68%.

*2.4.2.5. 7-Methyl-4-phenyl-2-(4-(trifluoromethyl)phenyl)-2H-pyrazolo[3,4-d]pyridazine (**8e**).* mp. 282 °C, IR (KBr) ν_{max}/cm^{-1}: 1594 (C=N), ^{1}H NMR (DMSO-d_6): δ 2.82 (s, 3H, CH_3), 7.39–8.19 (m, 9H, ArH's), 8.69 (s, ^{1}H-pyrazole), ^{13}C NMR (DMSO-d_6): δ 17.42, 111.23, 121.11,121.12, 122.56, 123.54,123.55, 125.16, 125.17, 128.45, 128.98, 130.54, 130.55, 131.08, 134.98, 138.65, 141.00, 149.23, 152.35. MS (*m*/*z*): 354 (M^+). Anal. Calcd for $C_{19}H_{13}F_3N_4$ (354.33): C, 64.40; H, 3.70; N, 15.81%. Found: C, 64.72; H, 3.56; N, 15.63%.

*2.4.2.6. 4-(4-Fluorophenyl)-7-methyl-2-(4-(trifluoromethyl)phenyl)-2H-pyrazolo[3,4-d]pyridazine (**8f**).* mp. >300 °C, IR (KBr) ν_{max}/cm^{-1}: 1592 (C=N), ^{1}H NMR (DMSO-d_6): δ 2.67 (s, 3H, CH_3), 7.51–7.89 (m, 8H, ArH's), 8.71 (s, ^{1}H-pyrazole), ^{13}C NMR (DMSO-d_6): δ 16.98, 110.87, 114.12, 114.13, 121.00,121.01, 122.54, 124.12,124.13, 126.00, 126.67, 128.16, 128.17, 128.98, 138.65, 141.14, 148.98, 152.02, 163.42. MS (*m*/*z*): 372 (M^+). Anal. Calcd 11 for $C_{19}H_{12}F_4N_4$ (372.32): C, 61.29; H, 3.25; N, 15.05%. Found: C, 61.58; H, 3.14; N, 14.87%.

3. Results and discussion

3.1. Catalytic regioselective 1,3-dipolar cycloaddition reaction of nitrilimines with enaminones

Solid basic catalysts, namely, MgO, Al_2O_3, KF/Al_2O_3, K_2CO_3 and Mg–Al HT were tested for the 1,3-DC reaction (Scheme 2) of the enaminone **3** with the nitrilimine **2a** (generated from the hydrazonoyl chloride **1a**).

The reaction was performed without solvent using solid base catalyst under microwave irradiation to obtain only one isolable product in each case (as examined by TLC and ^{1}H NMR spectroscopy).

To investigate the reactivity of hydrazonoyl hydrochlorides **2a–c** with enaminone derivatives, *E*-3-(dimethylamino)-1-phenylprop-2-en-1-one (**3a**) was used as the model dipolarophile substrates. *E*-3-(dimethylamino)-1-phenylprop-2-en-1-one was allowed to react with various aromatic hydrazonoyl hydrochlorides **2a–c** bearing various substituents to the nitrilimine group. The 1,3-DC reaction smoothly proceeded to give the corresponding pyrazole derivative in good yields (14–94%, see the entries 1–6 in Table 1).

Table 1
The yield of pyrazole derivative **5a** obtained using various solid base catalysts under microwave irradiation.

Entry	Catalyst	Time (min)	Yield[a] (%)
1	None	>90	0
2	Basic alumina	59	82
3	KF/basic alumina	40	58
4	K_2CO_3	>60	14
5	MgO	7	91
6	Mg–Al HT	4	94

[a] MW power: 330 W; reaction temperature 120 °C.

The results are indicating that Mg–Al HT catalyst offered the higher yield of the desired product (94%) within very short reaction time (4 min) under microwave irradiation. The next best catalyst is MgO, which offered 91% yield within 7 min, but we were unable to recover the catalyst from the reaction mixture, probably MgO might reacted with HCl (byproduct in the reaction) to form undesirable $MgCl_2$ salt. To further show the significance of this work, the catalytic activity of Mg–Al HT is compared with activity of triethylamine (frequently used homogeneous catalyst in the literature). The yield of pyrazole derivative **5a** is around 80%, when we used triethylamine as a catalyst at the same reaction conditions. This result is indicating that Mg–Al HT not only offering better catalytic activity but also green in nature. The reaction product was identified as the pyrazole structure **5a** in all cases, although there were two regioisomeric cycloadducts **5a** and **7a** seemed possible (Scheme 2).

However, the regioisomer **5a** was assigned for the reaction products on the basis of its ^{1}H NMR spectrum, in which, in the pyrazole ring system, C-4 is the most electron-rich carbon; thus, H-4 is expected to appear at a higher field, typically at δ 5–6 region. On the other hand, H-5 is linked to a carbon attached to a nitrogen atom and therefore, it is deshielded and appeared typically in the region δ 7.5–9.5. The ^{1}H NMR spectra of the isolated reaction product revealed, in each case, a singlet signal in the region of δ 8.68–9.67 as well as the absence of any signals around δ 5–6 ppm, which indicates the presence of the pyrazole H-5 rather than H-4 in the structure of the isolated product. These facts confirm the existence of regioisomer **5a** and rules out the other alternative structure **7a**. Unambiguous structure determination of the obtained products is therefore crucial to rationalize the observed regioselectivity. Structure elucidation was conveniently achieved on the basis of the long-range C–H connectivities (gHMBC 100 spectra) showed by pyrazole proton toward two C=O. On this basis, the analysis of gHMBC spectra of the product led us to attribute the signal at δ 195.75 ppm to the quaternary carbon (carbonyl group) owing to its correlation peaks with the pyrazole proton at δ 8.11 ppm; on the other hand, the signal at δ 189.94 ppm is attributed to the other carbonyl carbon owing to its correlation peak with the signal at δ 2.69 ppm easily assigned to the methyl group protons of the acetyl group. This observation indicating that only one carbonyl functional group correlate to the pyrazole proton which in accordance to the

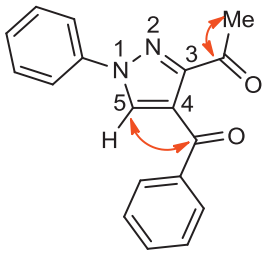

Fig. 2. Diagnostic correlations in the gHMBC (red arrows) in compounds **5a**. (For interpretation of the references to color in this figure legend, the reader is referred to the web version of the article.)

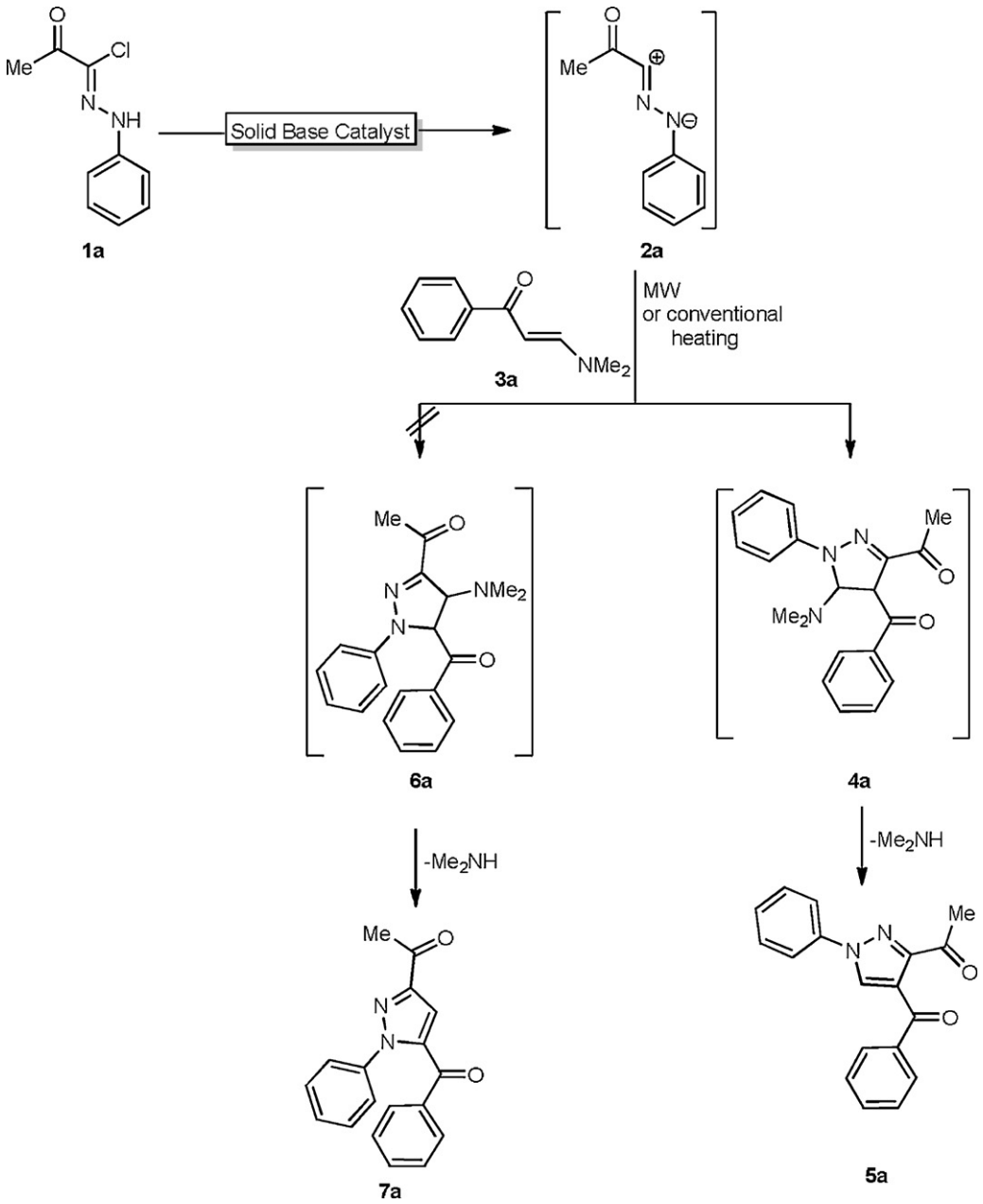

Scheme 2. Regioselective synthesis of pyrazole derivative **5a** using various solid base catalysts.

structure **5a** (Fig. 2), therefore these results confirm the existence of regioisomer **5a** and rules out the other alternative structure **7a**. The reaction product was identified as the pyrazole structure **5a** (Scheme 2) which was assumed to be formed via initial 1,3-DC of the nitrilimine **2a** to the activated double bond in the enaminone **3a** to afford the non-isolable dihydropyrazole intermediate **4a** followed by elimination of dimethylamine yielding the pyrazole derivative **5a**. In order to study the advantage of microwave irradiation on the rate of 1,3-DC reaction, the previously mentioned reaction was carried out by conventional electrical heating using Mg–Al HT as catalyst (Table 2).

The conventional heating method in oil bath needed 8 h to obtain 75% yield of the product. The obtained results revealed that the reactions required longer time to attain considerable yields under conventional heating methods and the yields are lower than that obtained using microwave protocol. From these results it is evident that microwave irradiation showed beneficial effect on 1,3-DC reaction in which it is possible to decrease the reaction time significantly from several hours to minutes with higher yields. We also performed the reactions without catalyst under both microwave and conventional methods and no reaction products were observed even after 90 min and 18 h under microwave and conventional heating, respectively.

Table 2
The yields of pyrazole derivatives **5a** using Mg–Al HT catalyst under conventional and microwave irradiations conditions.

Catalyst	Microwave condition		Conventional condition	
	Time (min)	Yield (%)	Time (h)	Yield (%)
None	>90	0	>20	0
Mg–Al HT	4	94	8	75

MW power: 330 W; reaction temperature: 120 °C.

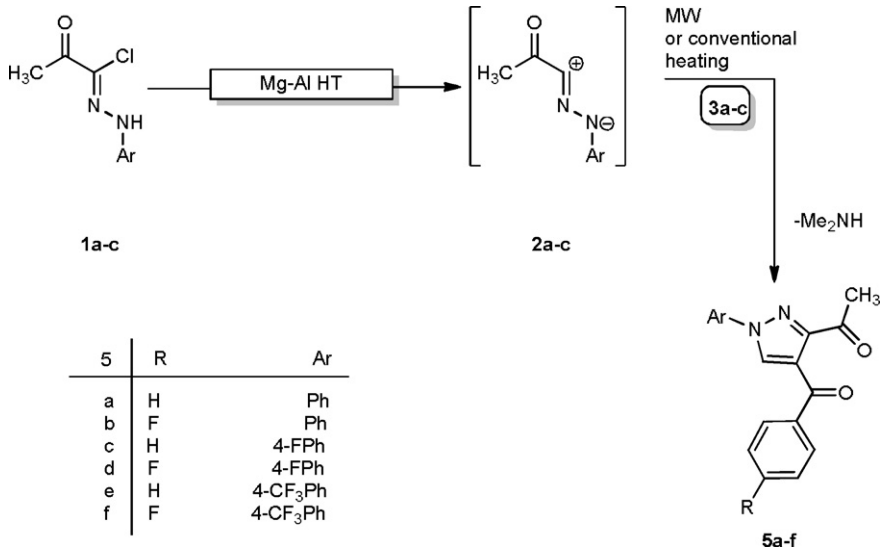

5	R	Ar
a	H	Ph
b	F	Ph
c	H	4-FPh
d	F	4-FPh
e	H	4-CF_3Ph
f	F	4-CF_3Ph

Scheme 3. Regioselective synthesis of pyrazole derivatives **5a–f** using Mg–Al HT catalyst.

The scope and generality of this protocol was tested by various derivatives of hydrazonyl halides **1b–c** as shown in the Scheme 3 under the optimized reaction conditions and corresponding pyrazole derivatives were obtained in excellent yields under microwave protocol (90–94%, Table 3).

The yields of pyrazole derivatives with trifluromethyl moiety (entries 5 and 6) are relatively lower than derivatives with simple fluorine group. This could be explained by the fact that trifluromethyl groups are highly hydrophobic in nature and might be repulsive to the reactive hydroxyl groups in the Mg–Al HT catalyst

Table 3
The efficiency of Mg–Al HT catalyst toward the synthesis of pyrazole derivatives **5a–f** under both conventional and microwave irradiations conditions.

Entry	Hydrazonyl chloride	Products	Microwave condition		Conventional condition	
			Time (min)	Yield (%)	Time (h)	Yield (%)
1	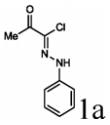 1a	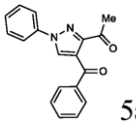 5a	4	94	8	75
2	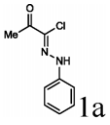 1a	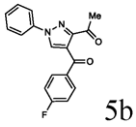 5b	4	92	8	75
3	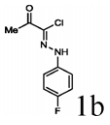 1b	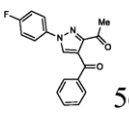 5c	5	92	8	75
4	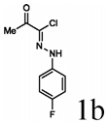 1b	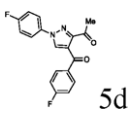 5d	5	91	9	76
5	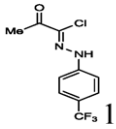 1c	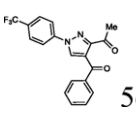 5e	6	90	8	75
6	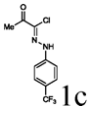 1c	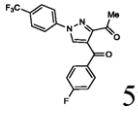 5f	6	90	8	75

MW power: 330 W; reaction temperature: 120 °C.

Table 4
The durability test of the Mg–Al HT catalyst toward the synthesis of pyrazole derivatives **5a–f**.

Compound No.	Number of successive uses of Mg–Al HT as catalyst					
	1st	2nd	3rd	4th	5th	
5a	4	4	4	4	5	
5b	4	4	4	4	5	
5c	5	5	5	5	6	Time to reach 100% conversion (min)
5d	5	5	5	5	7	
5e	6	6	6	7	7	
5f	6	6	6	7	7	

and also the effect of electron withdrawing ability of trifluromethyl group cannot be ignored for low activity. It was observed that the percentage yield was low under conventional heating conditions and the reaction time increased greatly. Again, microwave irradiation showed beneficial effect on 1,3-DC reaction in terms of reaction time and percentage yields. The reusability of the Mg–Al HT catalyst was checked for several reaction cycles under microwave irradiation, the catalyst removed after the completion of the reaction by filtration, washed with hot ethanol and dried under *vacuo*. The recovered catalyst was reused for five times using the same reaction conditions under microwave irradiation.

Table 4 shows that the regenerated catalyst performs the reactions efficiently under the same reaction conditions even after being used for five times. The slight decay observed in the catalytic activity of the Mg–Al HT catalyst on the fourth and fifth time and the decay of activity could be attributed to the weight loss of the catalyst during the working up in each time. These results are indicating the microwave stability and robust nature of the Mg–Al HT catalyst for 1,3-DC reaction.

A further confirmation of the regioselective synthesis of pyrazoles **5a–f** (not other regioisomer **7**) comes from its reaction with hydrazine hydrate under both microwave and conventional condition to afford a yellow-colored product, which was identified as the pyrazolo[3,4-*d*]pyridazine **8a–f** (Scheme 4 and Table 5). The microwave protocol offered 85% to 90% yields in 3 min, but the conventional heating method needed 120 min to offer 73% of yield. The IR spectra of compounds **5a–f** showed two carbonyl absorption bands, which were disappeared in the IR spectrum of the pyrazolo[3,4-*d*]pyridazine products **8a–i**. In addition to the IR data, ^{1}H, ^{13}C NMR and mass spectra results are in complete agreement with structure **8a–f**. All reaction times were determined by following the reaction progress via thin layer chromatography (TLC) and all products obtained were determined by elemental analyses, NMR, IR and mass spectroscopy data. These results are clearly indicating that microwave technology for heating has been shown to be more energy efficient than conventional method. Microwave irradiation is rapid and volumetric with the whole material heated simultaneously. In contrast, conventional heating is slow and the heat is introduced into the sample from the surface.

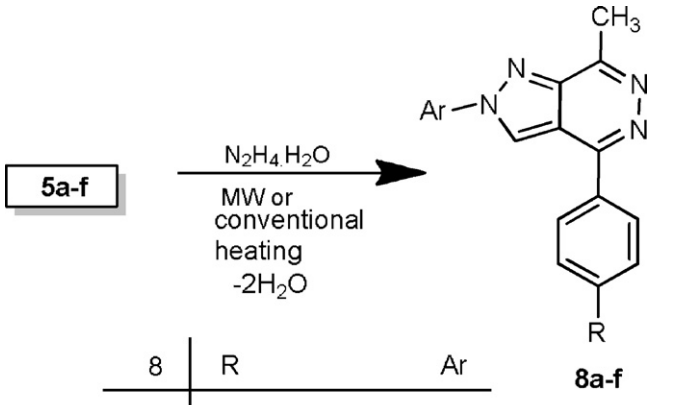

8	R	Ar
a	H	Ph
b	F	Ph
c	H	4-FPh
d	F	4-FPh
e	H	4-CF_3Ph
f	F	4-CF_3Ph

Scheme 4. Synthesis of pyrazolo[3,4-*d*]pyridazine **8a–f** derivatives.

3.2. Catalyst characterization

A through characterization of fresh and used catalysts was performed to understand the role of Mg–Al HT structure in the catalytic activity for 1,3-DC reaction. XRD patterns of the fresh and used catalysts after 1st run and 5th run are shown in Fig. 3. As synthesized catalyst shows characteristic (0 0 3), (0 0 6), (0 0 9) and (1 1 3) reflections at $2\theta = 11.4$, 22, 35, and 61.8° corresponding to Mg–Al HT [28] with formula $Mg_6Al_3(OH)_6CO_3{\cdot}4H_2O$.

The XRD patterns of used catalysts are very similar and shown different reflections due to a new phase. Removal of interlayer carbonate ions after the reaction evidenced by the shifting and broadening of the reflections and this less crystalline phase can be considered as meixnerite HT with formula of $Mg_6Al_2(OH)_{18}{\cdot}4H_2O$. Dehydroxylation and decarbonation of HTs into $Mg(Al)O_x$ mixed oxides and reconstruction of mixed oxides into HT analog after exposure water was observed by many research groups [29].

In the present study, the formation of meixnerite phase could be explained the fact that the carbonate ions in the pure Mg–Al HT are reacting with the HCl which is formed during the reaction. It is possible that the formed meixnerite could have HCO_3^- ions as compensating anions in the interlayer instead of the original carbonate ions. It is interesting to note that reflections due to magnesium chloride or aluminum chloride crystal structures were not observed and this observation revealing that HCl is not reacting with the metal ions, but with the interlayer anions. For further understanding of structural reorganization of the Mg–Al

Table 5
Synthesis of pyrazolo[3,4-*d*]pyridazine under microwave and conventional procedures.

Compound No.	Microwave condition		Conventional condition	
	Time (min)	Yield (%)	Time (min)	Yield (%)
8a	3	89	60	78
8b	3	90	60	80
8c	3	85	60	73
8d	3	88	60	76
8e	3	89	120	73
8f	3	88	120	71

MW power: 330 W; reaction temperature: 120 °C.

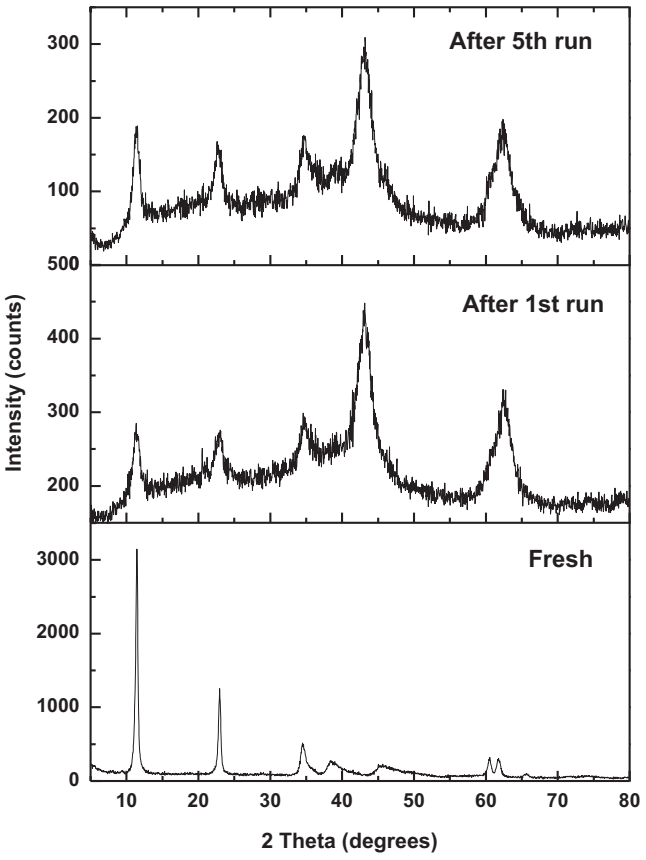

Fig. 3. XRD patterns of fresh and used catalysts.

HT, we analyzed the samples with FTIR and Raman spectroscopy methods.

Fig. 4 shows the FTIR spectra of fresh and spent Mg–Al HT catalysts after 1st and 5th catalytic runs. All the spectra were characterized with stretching vibrations of interlayer carbonate ions at 1355 cm^{-1}, along with the O—H stretching of the hydroxyl group and deformation vibration of H_2O at 3450 cm^{-1}. The peak at 1637 cm^{-1} in all the samples can be attributed to the bending mode of the interlayer water [30]. In the region of the spectra below 1000 cm^{-1} the lattice absorption bands, which can be assigned to the Al—O (around 755 cm^{-1}) and Mg—O (around 645 cm^{-1}) stretching modes [31]. It is interesting to note that the intensity of all the peaks due to interlayer ions and metal-oxygen bonds are decreasing with the increase of number of runs. This might be due

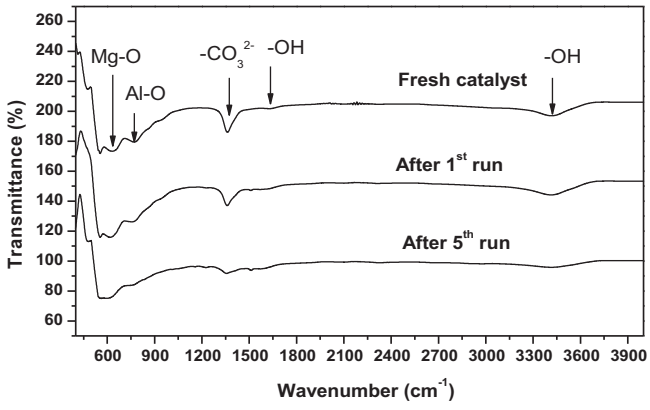

Fig. 4. FTIR spectra of fresh and used catalysts.

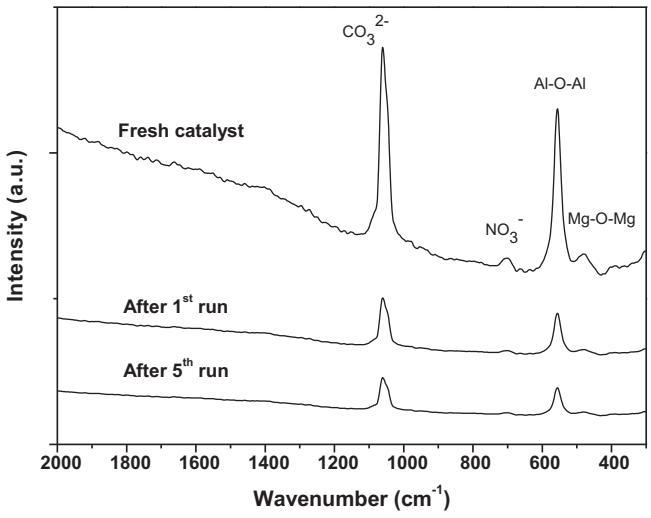

Fig. 5. Raman spectra of fresh and used catalysts.

to the fact that the formed HCl (bi-product of dehydrohalogenation of hydrazonoyl chlorides) could be reacting with interlayer anions.

Structural analysis of the catalysts was further studied by Raman spectroscopy. The Raman spectra of the fresh and spent catalysts were shown in Fig. 5. The presence of CO_3^{2-} and NO_3^- ions is reflected by sharp bands around 1063 cm^{-1} and 716 cm^{-1}, respectively. In the lower region, the two bands at around 471 cm^{-1} and 548 cm^{-1} are appeared in all three spectra. These bands were considered to be due to the linkage bonds, such as Mg—O—Mg and Al—O—Al linkage in the HT layers respectively [32]. The intensities of all bands showed significant decrease upon the increase of number of runs confirming the HT structural damage due to interaction with the evolved HCl. The confirmation of presence of intercalates carbonate ions from FTIR and Raman analyses revealing that HCO^{3-} ions are compensating with the carbonate ions.

Fig. 6 shows the N_2 adsorption–desorption isotherms and the pore size distribution patterns (in the inset) of fresh and used catalysts. The fresh Mg–Al HT sample exhibited type-II isotherm which was typical of mesoporous materials and slit shaped pores based on the Brunauer, Deming, Deming and Teller (BDDT) classification [33]. The sample was found to exhibit type B hysteresis loop (based on the De Boer idealization). The designation type-II was not withstanding the hysteresis loop, which normally corresponds to the type-IV model, because there was no plateau at high P/Po values. This isotherm was characteristic of clay minerals either of the cationic or anionic type such as hydrotalcites [34].

The adsorption–desorption isotherms of type-IV were observed for the used catalyst samples. A mesoporous structure based on the BDDT classification was observed. Both of the samples showed hysteresis loop type-A, indicative of cylindrical pores based on the De Boer idealization. The pore size distribution pattern of fresh sample shows unimodal pore distribution with single peak around 100 Å.

However, a bimodal distribution with two peaks at 8 Å and 100 Å was observed for used samples. The different surface properties for the re-used samples could be related to some disaggregation of the HT layers due to some atomic level overheating during microwave treatment at the reaction conditions used for the reactions. This gives to the formation of surface-defective sites which are responsible for the new porosity and the decrease in the surface area could be attributed to the pore blockage by a small amount of insoluble coke species. In order to obtain information about the basicity of the samples, we used the CO_2-TPD technique. The CO_2-TPD

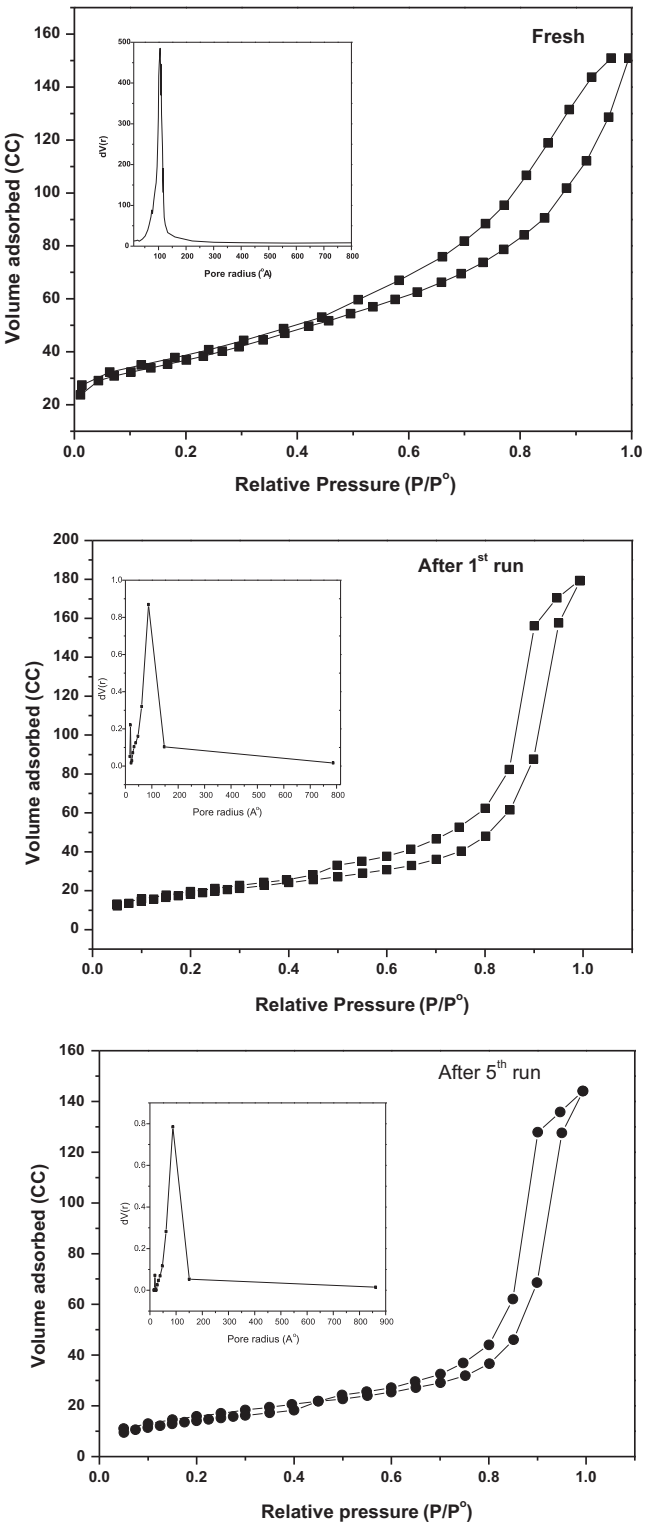

Fig. 6. N_2 isotherms and pore size distribution patterns of fresh and used catalysts.

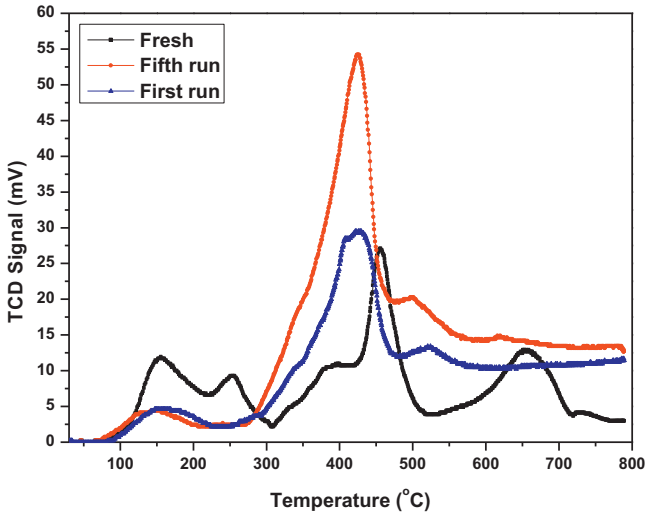

Fig. 7. TPD patterns of fresh and used catalysts.

patterns of the catalysts are shown in Fig. 7. CO_2 uptake is related to several types of basic sites and is caused by different types of carbonate coordination in the interlayer space of HTs. It is known that several types of species such as mono-dentate, bi-dentate and bicarbonate anions usually formed during the saturation of CO_2 with HTs [35]. Mono-dentate and bi-dentate carbonate formation involves low-coordination oxygen anions and are therefore considered as strong basic sites and the formation of bicarbonate anions requires surface hydroxyl groups [36]. The fresh Mg–Al HT sample showed total five desorption peaks. The low temperature peaks at 150 °C, 260 °C and 400 °C are due to the desorption weakly bounded CO_2 and decomposition of residual carbonate ions presented in the Mg–Al HT sample. A similar observation was made by Abello et al. [37] when they performed the blank test on the Mg–Al HT. The fresh catalyst also showed two main desorption peaks at 460 °C and 660 °C. The first peak was mainly attributed to bicarbonate groups formed by the interaction of CO_2 with hydroxyl groups in the Mg–Al HT and the second peak was tentatively attributed to the formation of strongly bonded surface metal carbonate species. The used catalysts showed a main desorption peak at 420 °C and a small peak between 510 and 520 °C. Diez et al. [38] reported that the desorption peak at about 420 °C can be attributed to the contribution of mainly bi-dentate carbonates species, together with bicarbonate species. The appearance of a peak at 540 °C is due to the presence of mono-dentate species. The results are demonstrating that all of the OH— sites are evaluated by CO_2-TPD experiments, but also that the OH— groups are still presented in the used samples are actually more accessible in structurally transformed Mg–Al HT catalyst. Moreover, the presence of the two peaks suggesting the existence of OH— groups with different strength. The differences in CO_2 uptake values between fresh and used catalysts can be attributed to the existence of irregularities or linear defects in the platelets of the microwave exposed samples. The consistent activity of the catalysts under microwave irradiation even after 5th recycle run with short reaction times can be explained by the fact that the Mg–Al HT catalyst is not decomposing into respective Mg and Al oxides under microwave irradiation and still possessed considerably high basic strength. As we observed the reactivity data in Table 1, Mg or Al oxides alone are unable to offer superior activity than Mg–Al HT catalyst.

3.3. *Regioselective 1,3-dipolar cycloaddition mechanism over Mg–Al HT catalyst*

A proposed mechanism for formation of the pyrazole derivative over Mg–Al HT catalyst is shown in Scheme 5. The first step is base induced dehydrohalogenation of the hydrazonoyl chloride under mild conditions to provide nitrilimine which produced 'in situ'. The second step involves the 1,3-dipolar cycloaddation reaction of nitrilimine with enaminone to produce the cycloadduct in a highly regioselective fashion. In the final step, the cycloadduct undergoes an elimination of–NMe_2 group by reacting with HCl

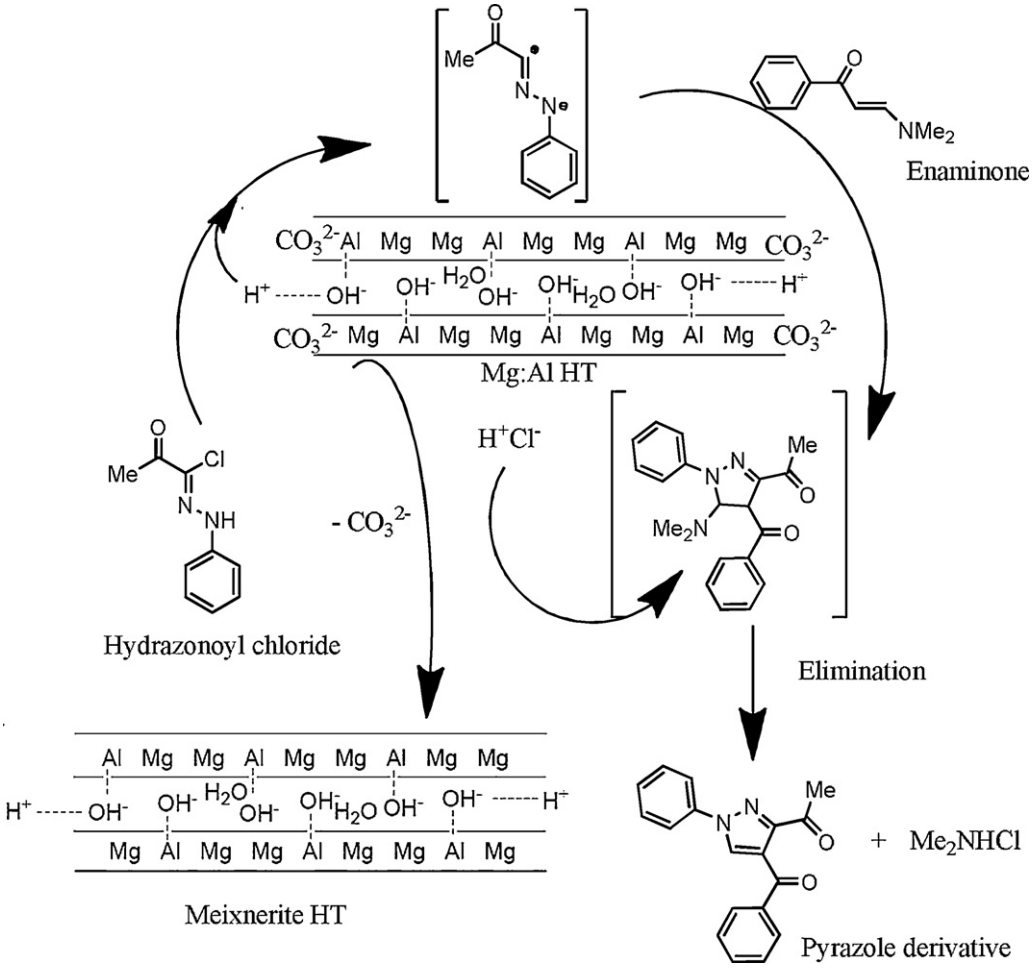

Scheme 5. Plausible regioselective 1,3-dipolar cycloaddition mechanism over Mg–Al HT catalyst.

at the pyrazoline ring affording pyrazole derivative. A simultaneous reaction between HCl and CO_3^{2-} ions presented in the Mg–Al HT causes the formation of meixnerite, analog of HT structure.

4. Conclusions

In summary, we report an efficient microwave assisted green protocol for regioselective 1,3-DC of nitrilimines with the enaminone derivatives over different base solid catalysts. Mg–Al HT catalyst showed a great advantage over all the investigated solid base catalysts. Microwave irradiation method offered high yields of pyrazole derivatives in very short reaction time over Mg–Al HT solid catalyst. A thorough catalyst characterization reveals that strong basic sites of the HTs are responsible for the consistent catalytic performance. Mg–Al HT maintained its structural and textural properties even after five catalytic runs, which appears crucial to obtain high yields of the product.

Acknowledgements

This project was funded by the Deanship of Scientific Research (DSR), King Abdulaziz University, Jeddah under Grant No. 32-130D1432. The authors, therefore, acknowledge DSR with thanks for their technical and financial support.

Appendix A. Supplementary data

Supplementary data associated with this article can be found, in the online version, at http://dx.doi.org/10.1016/j.molcata.2012.11.009.

References

[1] S. Fustero, M. Sanchez-Rosell, P. Barrio, A. Simn-Fuentes, Chem. Rev. 111 (2011) 6984.
[2] X.H. Liu, P. Cui, B.A. Song, P.S. Bhadury, H.L. Zhu, S.F. Wang, Bioorg. Med. Chem. 16 (2008) 4075.
[3] H. Foks, D. Pancechowska-Ksepko, A. Kedzia, Z. Zwolska, M. Janowiec, E. Augustynowicz-Kopec II, Farmaco 60 (2005) 513.
[4] A.M. Gilbert, A. Failli, J. Shumsky, Y. Yang, A. Severin, G. Singh, W. Hu, D. Keeney, P.J. Petersen, A.H. Katz, J. Med. Chem. 49 (2006) 6027.
[5] A.H. Shamroukh, M.E.A. Zaki, E.M.H. Morsy, F.M. Abdel-Motti, F.M.E. Abdel-Megeid, Arch. Pharm. Chem. Life Sci. 340 (2007) 345.
[6] O. Prakash, R. Kumar, V. Parkash, Eur. J. Med. Chem. 43 (2008) 435.
[7] R. Storer, C.J. Ashton, A.D. Baxter, M.M. Hann, C.L.P. Marr, A.M. Mason, P.L. Myers, S.A. Noble, H.R. Penn, N.G. Weir, G. Niall, J.M. Woods, P.L. Coe, Nucleotides 18 (1999) 203.
[8] M.J. Genin, C. Biles, B.J. Keiser, S.M. Poppe, S.M. Swaney, W.G. Tarpley, Y. Yagi, D.L. Romero, J. Med. Chem. 43 (2000) 1034.
[9] G. Daidone, B. Maggio, S. Plescia, D. Raffa, C. Musiu, C. Milia, G. Perra, M.E. Marongiu, Eur. J. Med. Chem. 33 (375) (1998) 21.
[10] S.A. Gamage, J.A. Spicer, G.W. Rewcastle, J. Milton, S. Sohal, W. Dangerfield, P. Mistry, N. Vicker, P.A. Charlton, W.A. Denny, J. Med. Chem. 45 (2002) 740.
[11] R.N. Comber, R.J. Gray, J.A. Secrist, Carbohydr. Res. 216 (1991) 441.
[12] A.M. Farag, A.S. Mayhoub, S.E. Barakat, A.H. Bayomi, Bioorg. Med. Chem. 16 (2008) 881.
[13] S.R. Donohue, C. Halldin, V.W. Pike, Tetrahedron Lett. 49 (2008) 2789.
[14] R. Huisgen, Angew. Chem. Int. Ed. 2 (1963) 565.

[15] (a) M.L. Kantam, V.S. Jaya, B. Sreedhar, M.M. Rao, B.M. Choudary, J. Mol. Catal. A: Chem. 256 (2006) 273;
(b) S. Chassaing, A.S.S. Sido, A. Alix, M. Kumarraja, P. Pale, J. Sommer, Chem. Eur. J. 14 (2008) 6713;
(c) K. Namitharan, M. Kumarraja, K. Pitchumani, Chem. Eur. J. 15 (2009) 2755;
(d) T. Katayama, K. Kamata, K. Yamaguchi, N. Mizuno, ChemSusChem 2 (2009) 59;
(e) N. Candelon, D. Lastcoures, A.K. Diallo, J.R. Aranzaes, D. Astruc, J.M. Vincent, Chem. Commun. (2008) 741.
[16] W.C. Tseng, L.Y. Wang, T.S. Wu, F.F. Wong, Tetrahedron 67 (2011) 5339.
[17] K. Yamaguchi, T. Oishi, T. Katayama, N. Mizuno, Chem. Eur. J. 15 (2009) 10464.
[18] G. Broggini, L. Garanti, G. Molteni, G. Zecchi, Heterocycles 45 (1997) 1945.
[19] B.F. Bonini, M.C. Franchini, D. Gentili, E. Locatelli, A. Ricci, Syn. Lett. 14 (2009) 2328.
[20] A.F. Hegarty, M.P. Cashman, F.L. Scott, J. Chem. Soc. Chem. Commun. (1971) 684.
[21] A. Lemos, J.A. Lourenco, Tetrahedron Lett. 50 (2009) 1311.
[22] F. Cavani, F. Trefiro, A. Vaccari, Catal. Today 11 (1991) 173.
[23] C.O. Kappe, Angew. Chem. Int. Ed. 43 (2004) 6250.
[24] H. Kaddar, J. Hamelin, H. Benhaoua, J. Chem. Res. (S) (1999) 718.
[25] (a) R.M. Shaaban, T.S. Saleh, A.M. Farag, Heterocycles 71 (2007) 1765;
(b) M.R. Shaaban, T.S. Saleh, A.S. Mayhoub, A.M. Farag, Eur. J. Med. Chem. 46 (2011) 3690;
(c) M.R. Shaaban, T.S. Saleh, A.S. Mayhoub, A. Mansour, A.M. Farag, Bioorg. Med. Chem. 16 (2008) 6344.
[26] (a) M. Mokhtar, T.S. Saleh, N.S. Ahmed, S.A. Al-Thabaiti, R.A. Al-Shareef, Ultrason. Sonochem. 18 (2011) 172;
(b) M. Mokhtar, T.S. Saleh, S.N. Basahel, J. Mol. Catal. A: Chem. 353–354 (2012) 122.
[27] M. Mokhtar, A. Inayat, J. Ofili, W. Schwieger, Appl. Clay Sci. 50 (2010) 176.
[28] J.C.A.A. Roelofs, D.J. Lensveld, A.J. van Dillen, K.P. deJong, J. Catal. 203 (2001) 184.
[29] (a) S. Abello, F. Medina, D. Tichit, J.J. Perez-Ramirez, J.C. Groen, J.E. Sueiras, P. Salagre, Y. Cesteros, Chem. Eur. J. 11 (2005) 728;
(b) K.K. Rao, M. Gravelle, J.V. Sanchez, F. Figueras, J. Catal. 173 (1998) 115;
(c) K.L. Erickson, T.E. Bostrom, R.L. Frost, Mater. Lett. 59 (2004) 226;
(d) J.C.A.A. Roelofs, A.J. van Dillen, K.P. de Jong, Catal. Lett. 74 (2001) 91.
[30] P. Kustrowski, D. Sulkowska, L. Chmielarz, A. Rafalska-Lasocha, B. Dudek, R. Dziembaj, Micropor. Mesopor. Mater. 78 (2005) 11.
[31] J.T. Kloprogge, R.L. Frost, Appl. Catal. A: Gen. 184 (1999) 61.
[32] J.T. Kloprogge, L. Hickey, R.L. Frost, Appl. Clay Sci. 18 (2001) 37.
[33] O. Bergada, I. Vicente, P. Salagre, Y. Cesteros, F. Medina, J.E. Sueiras, Micropor. Mesopor. Mater. 101 (2007) 363.
[34] F. Prinetto, G. Ghiotti, P. Graffin, D. Tichit, Micropor. Mesopor. Mater. 39 (2000) 229.
[35] R.J. Chimentao, S. Abello, F. Medina, J. Llorca, J.E. Sueiras, Y. Cesteros, P. Salagre, J. Catal. 252 (2007) 249.
[36] F. Prinetto, G. Ghiotti, R. Durand, D. Tichit, J. Phys. Chem. B 104 (2000) 1117.
[37] S. Abello, F. Medina, D. Tichit, J. Perez-Ramirez, X. Rodriguez, J.E. Sueiras, P. Salagre, Y. Cesteros, Appl. Catal. A: Gen. 281 (2005) 191.
[38] V.K. Diez, C.R. Apesteguia, J.I. Di Cosimo, J. Catal. 215 (2003) 220.